Pergamon

*Int. J. Solids Structures* Vol. 34, No. 24, pp. 3085–3098, 1997
© 1997 Elsevier Science Ltd
All rights reserved. Printed in Great Britain
0020–7683/97 $17.00 + .00

PII: S0020–7683(96)00175–8

# CRACK DEFLECTION IN FUNCTIONALLY GRADED MATERIALS

PEI GU and R. J. ASARO
Department of Applied Mechanics and Engineering Sciences, Mail Code 0411,
University of California at San Diego, 9500 Gilman Drive, La Jolla, CA 92093-0411, U.S.A.

(*Received* 18 *April* 1996; *in revised form* 7 *August* 1996)

**Abstract**—Small crack deflection in brittle functionally graded materials (FGMs) is studied. The FGMs are modeled as simply nonhomogeneous materials, i.e., the effect of microstructure is neglected and the material property variation is considered to be continuous. Considering local homogeneity and the small scale inelasticity of brittle materials, the toughness is taken to be independent of direction; therefore, the crack propagates along the direction of maximum energy release rate, or the direction which gives a vanished mode II stress intensity factor. Kink directions for several specimens which may be used to experimentally study fracture behavior of FGMs are calculated. It is shown that material gradients have a strong effect on the kink direction when the crack is at the central region of a FGM, whereas they have little effect when the crack is close to the boundaries of the FGM. © 1997 Elsevier Science Ltd.

## 1. INTRODUCTION

In functionally graded materials (FGMs), although the absence of sharp interfaces does largely reduce material property mismatch, cracks occur when they are subjected to external loadings (Yamanouchi *et al.*, 1990; Holt *et al.*, 1993). Fractures induced by these cracks may in large part determine the overall mechanical and thermal-mechanical responses of FGMs. The need to understand, quantify and improve the toughness of FGMs has brought interest in a fracture mechanics methodology for such materials. In our recent work (Gu and Asaro, 1997), stress intensity factors of several specimens composed of FGMs were solved; the effect of material gradients on near-tip fields was determined; and possible fracture criterion was discussed. In this paper, we address crack deflection (or kinking) in brittle FGMs, i.e., for crack with arbitrary orientation, we study the direction of its extension when the critical condition is met. Here, brittle FGMs are those having strictly linear response. An example is the Si-C FGM system in which both material phases are brittle. For those FGMs made of metal and ceramic phases, the present model gives an approximate solution if the crack is on the brittle-behaved ceramic-rich side. If the crack is at the metal-rich side, its propagation is primarily via plastic mechanisms. Our study aimed at non-linear crack tip behavior is ongoing (Gu and Asaro, 1996), and will be discussed elsewhere.

The crack deflection model is developed in the same spirit as that for homogeneous materials (Cotterell and Rice, 1980) and for bimaterials with interface cracks (He and Hutchinson, 1989). The crack tip stress and displacement fields of FGMs, as briefly discussed in Section 2, take the same forms as those for homogeneous materials. Based on this fact, the asymptotic problem, which has a homogeneous body, is employed to study the crack tip behavior. Considering the local homogeneity and small-scale inelasticity of brittle materials around the crack tip, the toughness is taken to be independent of direction at a fixed point. It follows that the crack propagates along the direction of maximum energy release rate or the direction in which the mode II stress intensity factor vanishes. The kink direction is a function of the external loading, the geometry, and elastic property's gradients of a given specimen. After a short discussion on crack deflection model for homogeneous materials and for bimaterials in Section 3.1 and Section 3.2, we present that for FGMs in Section 3.3, in which the asymptotic problem based on the K-field and the directional independence of the toughness are discussed in detail. Kink angles for four-point bending

specimen, double-cantilever beam and center cracked plate are calculated in Section 4, and the following qualitative results are obtained from the solution. For the four-point bending specimen, the crack intends to grow to the more compliant side. For the double-cantilever beam and center cracked plate, when the crack is at the middle of the specimen or at the compliant side, it intends to grow to the more compliant side, whereas when the crack is at the stiff side it intends to grow to the stiffer side. The material gradients do have a strong effect on the kink angle when the crack is at the middle of the FGM; but the effect is small when the crack is close to the boundaries of the FGM. We also investigate crack propagation in a compositionally graded interface. It is found that of the two Dundurs' parameters, $\alpha$ and $\beta$ (see eqn 12), the effect of the former on the kink angle is stronger than the latter.

## 2. CRACK TIP FIELDS OF FGMs

For the purpose of studying crack kinking, the major results of the crack tip fields in FGMs are highlighted; detailed discussion can be found in Gu and Asaro (1997). The functionally graded material shown in Fig. 1 is considered as a nonhomogeneous material whose material properties vary continuously. Stresses near the crack tip have a square-root singularity, and singular terms of the stresses are of the form:

$$\sigma_{ij} = \frac{K_I}{\sqrt{2\pi r}}\bar{\sigma}_{ij}^{I}(\theta) + \frac{K_{II}}{\sqrt{2\pi r}}\bar{\sigma}_{ij}^{II}(\theta) + \frac{K_{III}}{\sqrt{2\pi r}}\bar{\sigma}_{ij}^{III}(\theta), \tag{1}$$

where $i, j = 1, 2, 3$; $r$ and $\theta$ are the polar coordinates shown in Fig. 1. The dimensionless angular functions $\bar{\sigma}_{ij}^{I}(\theta)$, $\bar{\sigma}_{ij}^{II}(\theta)$ and $\bar{\sigma}_{ij}^{III}(\theta)$ are the same as those for homogeneous materials. The result is independent of the form for material properties and the orientation of the crack. The stress intensity factors $K_I$, $K_{II}$ and $K_{III}$ are functions of the material gradients, external loading, and geometry. Material gradients do not affect the order of the singularity and the angular functions, but do affect the stress intensity factors. As a result the near-tip stresses have the same form as that for a homogeneous material. It can also be shown that the near-tip displacements take the same form as that for homogeneous materials, and this is independent of material gradients and the orientation of the crack. For plane stress and plane strain problems, they are of the form:

$$u_i = \frac{K_I}{2E'(0)}\sqrt{\frac{r}{2\pi}}u_i^{I}(\theta) + \frac{K_{II}}{2E'(0)}\sqrt{\frac{r}{2\pi}}u_i^{II}(\theta), \tag{2}$$

where $E'(0)$ is the Young's modulus at the crack tip, and the angular functions, $u_i^{I}(\theta)$ and $u_i^{II}(\theta)$, are the same as those for homogeneous materials.

Having the near tip stress and displacement fields, the energy release rate of the crack tip is obtained as

$$\mathcal{G} = \frac{K_I^2}{E'(0)} + \frac{K_{II}^2}{E'(0)} + \frac{K_{III}^2}{2\mu(0)}. \tag{3}$$

Here, $\mu(0)$ is the shear modulus at the crack tip. The above equation is again independent

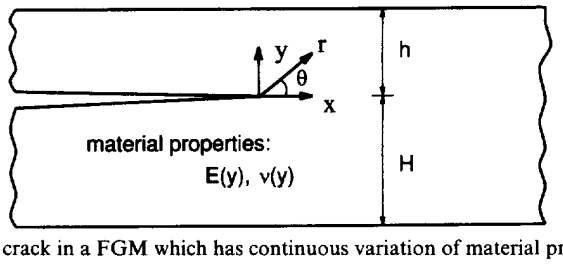


Fig. 1. A crack in a FGM which has continuous variation of material properties.

of the form for the material properties and the orientation of the crack, and has the same form as that for homogeneous materials. The path-independence of the $J$ integral (Rice, 1968) holds if the crack is perpendicular to the direction along which material properties change; this is implied in Rice's original proof for homogeneous materials. Using the near tip fields obtained above, it can be shown that the $J$ integral is equal to the energy release rate for the crack perpendicular to the direction along which material properties change.

For in-plane problems, the complex stress intensity $K = K_I + iK_{II}$ for FGMs has the following generic form

$$K = |K| e^{i\psi}, \tag{4}$$

where

$$\psi = \tan^{-1} \frac{K_{II}}{K_I} \tag{5}$$

is the phase angle of the complex stress intensity factor. The phase angle measures mode mixity, i.e., the proportion of the shear traction to the normal traction ahead of the crack tip, since

$$\psi = \tan^{-1} \left( \frac{\sigma_{xy}}{\sigma_{yy}} \right)_{\theta=0, r\to 0}. \tag{6}$$

The complex stress intensity has the following dimensional form:

$$K = TL^{1/2} Y, \tag{7}$$

where $T$ is a representative stress magnitude, $L$ is a characteristic length and $Y$ is a dimensionless function which relates to the geometry of the problem and material properties. Both the phase angle and the dimensional form are consistent with those for homogeneous materials.

## 3. MODELING OF CRACK DEFLECTION

A number of studies have been performed for crack deflection in homogeneous materials and bimaterials with interface cracks. Before discussing the model for FGMs, we give a brief review of some results for homogeneous materials and bimaterials in Section 3.1 and 3.2, respectively. Since the interest is crack extension initiation, we concentrate on small kinks, where the kink length is much less than the length of the pre-existing cracks (main cracks).

### 3.1. *Homogeneous materials*

Stress intensity factors at the kinked crack tip uniquely characterize its near-tip fields; therefore, they are the parameters to determine the deflection direction at the load when the crack starts to propagate. The stress intensity factors for the kinked crack in a homogeneous material have been solved for elsewhere, including Palaniswamy and Knauss (1978) and Lo (1978). The latter detailed a method for solving crack kinking problems using integral equations which are formulated by the continuous distribution of dislocations: a method valid for both finite and infinitesimal (small) kinks. The idea is essentially to remove the tractions which are caused by the stress field of the main crack in the kinked crack before kinking. For the infinitesimal kink, since the kink length is much smaller than the size of the K-dominance zone of the main crack, the loading is the two stress intensity factors, $K_I$ and $K_{II}$, of the main crack, and the stress intensity factors of the kinked crack, $K_I^*$ and $K_{II}^*$, are obtained in terms of $K_I$ and $K_{II}$. This is the asymptotic problem: a semi-infinite crack in the homogeneous material which is loaded by the K-field of the main crack characterized by $K_I$ and $K_{II}$; the propagation of the main crack is controlled by its K-field. At large

distances from the semi-infinite crack tip, the stress field approaches the K-field of the main crack. Near the semi-infinite crack tip, the stress field is perturbed from the K-field of the main crack because of the kinking. By dimensional analysis and linearity, the stress intensity factors of the kinked crack are expressed as

$$K_I^* = C_{11}(\phi)K_I + C_{12}(\phi)K_{II},$$
$$K_{II}^* = C_{21}(\phi)K_I + C_{22}(\phi)K_{II}, \tag{8}$$

where $\phi$ is the angle between the kink direction and the main crack, and $C_{11}$, $C_{12}$, $C_{21}$ and $C_{22}$ are coefficients which can be determined by Lo's method. For finite kinks, $K_I^*$ and $K_{II}^*$ must be obtained by solving a full boundary value problem considering the load, the geometry of the specimen including both the main crack length and the kink length.

If there is only mode I loading, the crack would extend along the direction of the pre-existing crack. This direction is the direction of maximum energy release rate. For mixed mode problems, the two often used criteria are the maximum energy release rate criterion (Cotterell, 1965) and mode I type criterion (also referred to as local symmetry criterion, see Cotterell and Rice (1980) and Goldstein and Salganik (1974)). The former states that the crack propagates along the direction of maximum energy release rate, and the latter that the crack grows along the direction for which the mode II stress intensity factor vanishes. Kink directions determined by the two criteria are consistent: it was shown that the difference is less than 1 degree for almost all loading combinations except the case in which the shear mode is overwhelmingly dominant where the difference is then about 2 degrees (He and Hutchinson, 1989).

For small $\phi$, using first order approximation, Cotterell and Rice (1980) were able to analytically evaluate those coefficients in (8) as

$$C_{11} = \frac{1}{4}\left(3\cos\frac{\phi}{2} + \cos\frac{3\phi}{2}\right),$$
$$C_{12} = -\frac{3}{4}\left(\sin\frac{\phi}{2} + \sin\frac{3\phi}{2}\right),$$
$$C_{21} = \frac{1}{4}\left(\sin\frac{\phi}{2} + \sin\frac{3\phi}{2}\right),$$
$$C_{22} = \frac{1}{4}\left(\cos\frac{\phi}{2} + 3\cos\frac{3\phi}{2}\right). \tag{9}$$

They showed that stress intensity factors calculated by using (9) are in good agreement with those exact solutions for $\phi$ up to 40 degrees: the error is less than 5%. They also showed that, by substituting the approximation (9) into (8), the energy release rate is locally a maximum for the mode I path (the path with a vanished mode II stress intensity factor).

### 3.2. *Bimaterials with interface cracks*

For an interface crack, stresses have an oscillatory singularity, and both stress intensity factors and angular functions involve Dundurs' parameters, i.e.,

$$\sigma_{ij} = \frac{\mathrm{Re}(Kr^{i\varepsilon})}{\sqrt{2\pi r}}\tilde{\sigma}_{ij}^{I}(\theta,\varepsilon) + \frac{\mathrm{Im}(Kr^{i\varepsilon})}{\sqrt{2\pi r}}\tilde{\sigma}_{ij}^{II}(\theta,\varepsilon) + \frac{K_{III}}{\sqrt{2\pi r}}\tilde{\sigma}_{ij}^{III}(\theta), \tag{10}$$

where $K = K_I + iK_{II}$, and

$$\varepsilon = \frac{1}{2\pi} \ln \frac{1-\beta}{1+\beta}. \tag{11}$$

In (10), $\beta$ is one of the two Dundurs' parameters. The Dundurs' parameters (Dundurs, 1969), $\alpha$ and $\beta$, are defined as

$$\alpha = \frac{\mu_1(\kappa_2+1)-\mu_2(\kappa_1+1)}{\mu_1(\kappa_2+1)+\mu_2(\kappa_1+1)},$$
$$\beta = \frac{\mu_1(\kappa_2-1)-\mu_2(\kappa_1-1)}{\mu_1(\kappa_2+1)+\mu_2(\kappa_1+1)}, \tag{12}$$

where $\mu_1$ and $\mu_2$ are the shear moduli of the two bulk materials; $\kappa_i = 3-4\nu_i$ for plane strain and $\kappa_i = (3-\nu_i)/(1+\nu_i)$ for plane stress ($i = 1, 2$), with $\nu_1$ and $\nu_2$ being the Poisson's ratios of the two bulk materials. The complex stress intensity factor, $K$, has the dimensional form

$$K = TL^{1/2-i\varepsilon}Y, \tag{13}$$

where $T$ is a representative stress magnitude, $L$ is a characteristic length and $Y$ is a dimensionless function which relates to the geometry of the problem and Dundurs' parameters.

For the interface crack kinking problem, the stress intensity factors of the kinked crack are not unique in the sense that they are dependent on the kink length. For small kinks, dimensional analysis and linearity give the relationship between the complex stress intensity factor of the kinked crack $K^*$ and that of the interface crack $K$ as

$$K^* = c(\phi, \alpha, \beta)Ka^{i\varepsilon} + \bar{d}(\phi, \alpha, \beta)\bar{K}a^{-i\varepsilon}, \tag{14}$$

where $a$ is the kink length and $(^-)$ denotes the conjugate of the complex variable. It is seen that only when $\beta = 0$ (i.e. $\varepsilon = 0$) $K^*$ is independent of the kink length. A complete solution in this case was obtained by He and Hutchinson (1989) using the integral equation method. The kink length dependence case, $\beta \neq 0$, was studied by Mukai *et al.* (1990) and Geubelle and Knauss (1994). The results showed that $K^*$ and the kink angle are strongly dependent on kink length for sufficiently large $\beta$. It was concluded by the latter that this is due to "rotational stress and deformation fields" (Symington, 1987) at the crack tip, which extended to a region far outside of the contact zone. They suggested that the kink length $a$ should be viewed as a property of the bimaterial combination, and be determined by fitting experimental data.

Whether the interface crack stays on the interface or kinks into one of the bulk materials is decided by the ratio of the energy release rate for the crack to extend on the interface $\mathcal{G}_i$ to that for the crack to kink $\mathcal{G}_s$, and the ratio of the interfacial toughness $\Gamma_i$ to the toughness of the bulk materials $\Gamma_s$. Kinking is thereby favored if

$$\frac{\mathcal{G}_s}{\mathcal{G}_i} > \frac{\Gamma_s}{\Gamma_i}. \tag{15}$$

### 3.3. *Functionally graded materials*

Crack propagation is the competition between the energy release rate and the toughness of the material. In order to address crack kinking in FGMs, we need to study both physical parameters.

The energy release rate of a kinked crack in a FGM depends on the geometry, the loading, and the material properties including material gradients. The exact solution for it has to be obtained from the solution of the full boundary value problem. For small kinks, the solution may be obtained in an asymptotic way similar to that outlined in Section 3.1. In Section 2, we have noted that crack tip fields for FGMs have the same forms as those

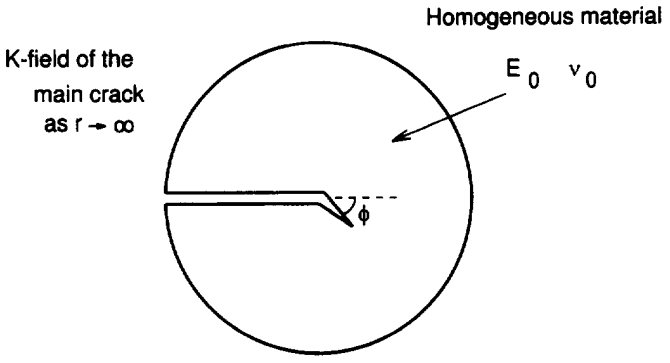


Fig. 2. Local homogenization near the crack tip region in a FGM: a homogeneous body is loaded far away from the tip of a semi-infinite crack by the K-field of the crack in the FGM (the asymptotic problem).

for homogeneous materials, and only the stress intensity factors are functions of material gradients. The elastic constants appeared in the displacement near-tip field and the energy release rate are those at the crack tip. This suggests that, to study crack kinking one can consider the asymptotic problem shown in Fig. 2: a homogeneous plate, which has a semi-infinite crack and the elastic constants at the main crack tip, is subjected to the loading characterized by the stress intensity factors of the main crack. The only difference between the asymptotic problem for FGMs and that for homogeneous materials is that here the elastic constants appearing in the problem are those at the main crack tip which change with its position, whereas for homogeneous materials those elastic constants do not change with the position of the main crack tip. Knowing the asymptotic problem, stress intensity factors of the kinked crack can be solved by the same technique to solve those for homogeneous materials. The local homogenization results in that the relationship (8) for homogeneous materials holds for FGMs. Specifically, the coefficients $C_{ij}$ in (8) are the same as those for homogeneous materials, and material gradients affect the stress intensity factors of the kinked crack $K^*$ only through the stress intensity factors of the main crack $K$. These coefficients can be obtained accurately by using the integral equation method to solve the asymptotic problem in Fig. 2, which is a homogeneous crack-kinking problem; as mentioned before, they are well approximated by the expressions in (9) for small $\phi$.

The above approach for crack kinking is valid if the kink length is sufficiently smaller than the size of K-dominance zone. To examine the K-dominance zone, the asymptotic solution over the full field solution ahead of the crack tip, $\sigma^a_{yy}/\sigma^f_{yy}$, is plotted in Fig. 3 for the center cracked plate subjected to remote stress shown in Fig. 4(d), where $h/H = 1$. It is assumed that the width of the plate is much larger than the crack length. The crack is perpendicular to the direction of material property variation, and the variation is in the exponential form which is the same as that in Gu and Asaro (1997) and which will also be stated in the next section. It is seen that the size of the dominance zone decreases as $\gamma$, which is the measure of material gradients, increases. At 10% of the crack length ahead of

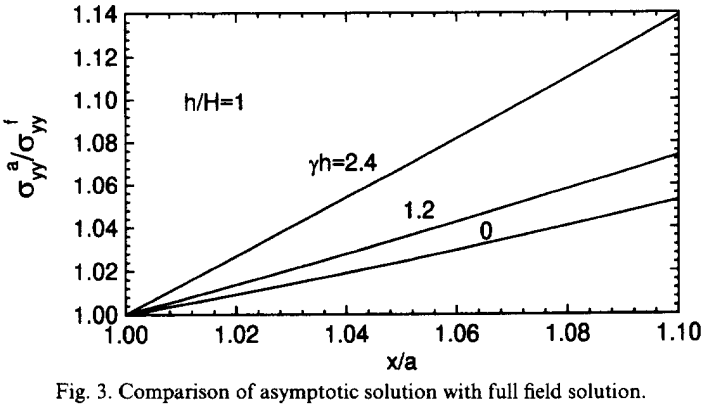


Fig. 3. Comparison of asymptotic solution with full field solution.

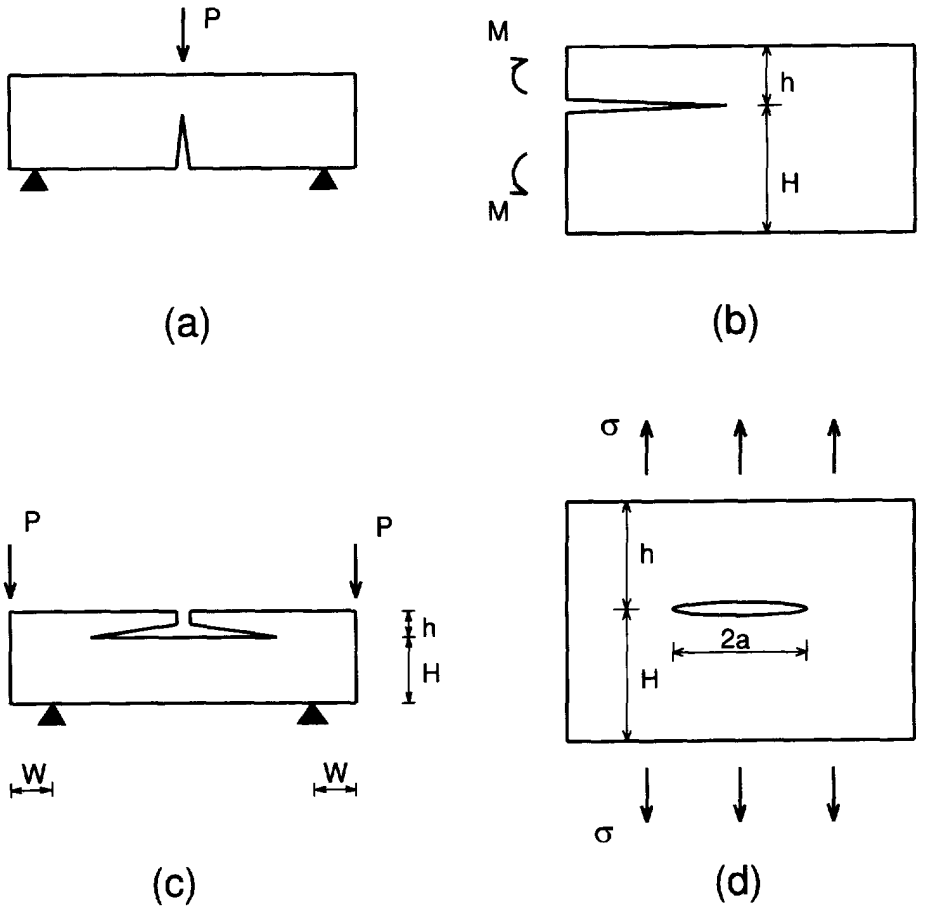


Fig. 4. Several Specimens. (a) Three-point bending specimen. (b) Double-cantilever beam. (c) Four-point bending specimen. (d) Center cracked plate. The material properties vary along the vertical direction.

the crack tip the error between the exact and asymptotic solutions for homogeneous materials is 5%, whereas it is 7% for $\gamma h = 1.2$, and 14% for $\gamma h = 2.4$. Note that, in the case of $\gamma h = 1.2$, the ratio of the Young's modulus at the upper boundary to that at the lower boundary is about 11. It is fair to say that, for material gradients which are not too large, the radius of K-dominance zone would be in the size comparable to that of homogeneous materials, at least, not reduced much from that of homogeneous materials. For interface cracks in bimaterials and sandwich structures, the size of the dominance zone was investigated by O'Dowd *et al.* (1992), Shih (1991) and Gu (1993).

The often used techniques to make FGMs are thermal spray, powder processing and chemical vapor deposition (CVD). The microstructure of these FGMs depends on these manufacturing processes (see Yamanouchi *et al.*, 1990; Holt *et al.*, 1993). For a real FGM, typical micrograph shows discrete structure. If the FGM is made of material phases A and B, the A-rich side has a dispersive structure with B particles in the A matrix; at the B-rich side A particles are in the B matrix; and in the middle region between the two sides, it is a skeletal structure due to the connectivity of both phases. For such complicated structure, the characterization of its toughness is an open issue at this moment. The toughness is likely a function of the position of the crack tip, and may also depend on the direction along which the crack propagates and the loading phase angle. In this study, we neglect the effect of microstructure; we study the idealized case, simply nonhomogeneous materials, i.e., the materials are those with a continuous change of material properties. This means that the microstructure of a FGM is sufficiently fine that the continuum model gives satisfactory predictions.

For the simply nonhomogeneous material, since we study small kink in the locally homogeneous body controlled by the K-field (the asymptotic problem shown in Fig. 2) and

small-scale inelastic deformation around the crack tip, the toughness of the non-homogeneous material is taken to be independent of direction at a fixed point. If the cohesive stress $p$, the inelastic stress in the cohesive zone ahead of the crack tip to restrain separation for creating free surfaces (Dugdale, 1960; Barenblatt, 1962) is not only a function of separation but also position, say $p(\delta, y)$, the toughness of the FGM at the position $y$ may be expressed as

$$\Gamma = \int_0^{\delta_0} p(\delta, y)\, \mathrm{d}\delta, \tag{16}$$

where $\delta_0$ is limit separation at $y$. This is the result of applying the $J$ integral around the cohesive zone of the homogeneous body in Fig. 2 (see Rice, 1968).

For some FGMs, their micrograph may show layered structures, and these discrete microlayers have varying compositions and thus form the macroscopic material gradients along the thickness direction. If the crack lies on one of the interfaces, it may behave like a real interface crack. The mechanics of elastic interface fracture was established (Rice, 1988; Hutchinson, 1990). The criterion for an interface crack to grow on the interface is

$$\mathscr{G} = \Gamma(\psi), \tag{17}$$

where $\psi$ is the phase angle. The condition for crack kinking into one of the two adjacent layers was stated in Section 3.2. Plastic interface fracture was investigated by Shih and Asaro (1988, 1989) and Shih (1991). In this study, since the FGM is considered as a simply nonhomogeneous material, the possibility of having discrete microlayers is excluded.

Considering the above, the kink direction for the FGM is the direction of maximum energy release rate or that in which the mode II stress intensity factor vanishes. Both directions relate to the geometry, loading and the material gradients. The two criteria for FGMs, like those for homogeneous materials, are also consistent, since they are built on locally homogeneous materials.

The locally homogenized model is expected to work well for brittle, simply non-homogeneous materials, as discussed above. For those FGMs in which plastic mechanisms are involved in a sufficiently large region around the main crack tip, or microstructural gradients are presented at the tip region, further investigation is needed to determine these effects.

## 4. SOLUTIONS AND IMPLICATIONS

An immediate consequence of the present model is that, for the three point bending specimen shown in Fig. 4(a), the crack extends vertically ahead of the main crack tip along its direction, since the crack tip only has a mode I stress intensity factor (both geometry and loading are symmetric). The conclusion is independent of the form of the material property variation, and is the same as that in the case of a homogeneous material.

Stress intensity factors for the double-cantilever beam, Fig. 4(b), and the four-point bending specimen, Fig. 4(c), were obtained by Gu and Asaro (1997), where material properties were assumed to follow the exponential form:

$$\begin{aligned} E'(y) &= E_0\, \mathrm{e}^{\gamma y}, \\ \nu'(y) &= \nu_0(1+\rho y)\, \mathrm{e}^{\gamma y}. \end{aligned} \tag{18}$$

In (18), $\gamma$ and $\rho$ are material constants representing the material gradients; $E_0$ and $\nu_0$ are the values of these elastic properties at $y = 0$. For plane stress problems, $E'(y) = E(y)$ and $\nu'(y) = \nu(y)$, where $E(y)$ and $\nu(y)$ are Young's modulus and Poisson's ratio, respectively; for plane strain problems, $E'(y) = E(y)/[1-\nu(y)^2]$ and $\nu'(y) = \nu(y)/[1-\nu(y)]$. The shear modulus, $\mu(y)$, relates to Young's modulus and Poisson's ratio by

$$\mu(y) = \frac{E'(y)}{2[1+\nu'(y)]}. \tag{19}$$

The above forms provide analytical flexibility and lead to somewhat simple forms for the field equations. Using (18) and (19), it is shown that for a traction boundary value problem, the stress field depends on the material parameter $\gamma$, which is related to the moduli at the upper boundary $E'_u$ and at the lower boundary $E'_l$ as

$$\gamma h = \frac{h}{L} \ln \frac{E'_u}{E'_l}. \tag{20}$$

In (20), $L = h + H$ is the thickness of the FGM and $h$ a characteristic length. The parameter $\rho$ in (18) does not affect the solution. When the modulus at the upper boundary is larger than that at the lower boundary, for example, the upper side is ceramic and the lower side is metal, the parameter $\gamma h$ is larger than zero; for the case of a homogeneous material, it is zero. We examine the kink direction in the double-cantilever beam and the four-point bending specimen.

For the double-cantilever beam, the energy release rate $\mathcal{G}$, normalized by $M/h^{1.5}$, is plotted vs the possible kink angle $\phi$ in Fig. 5, where $\phi$ is positive when the crack goes

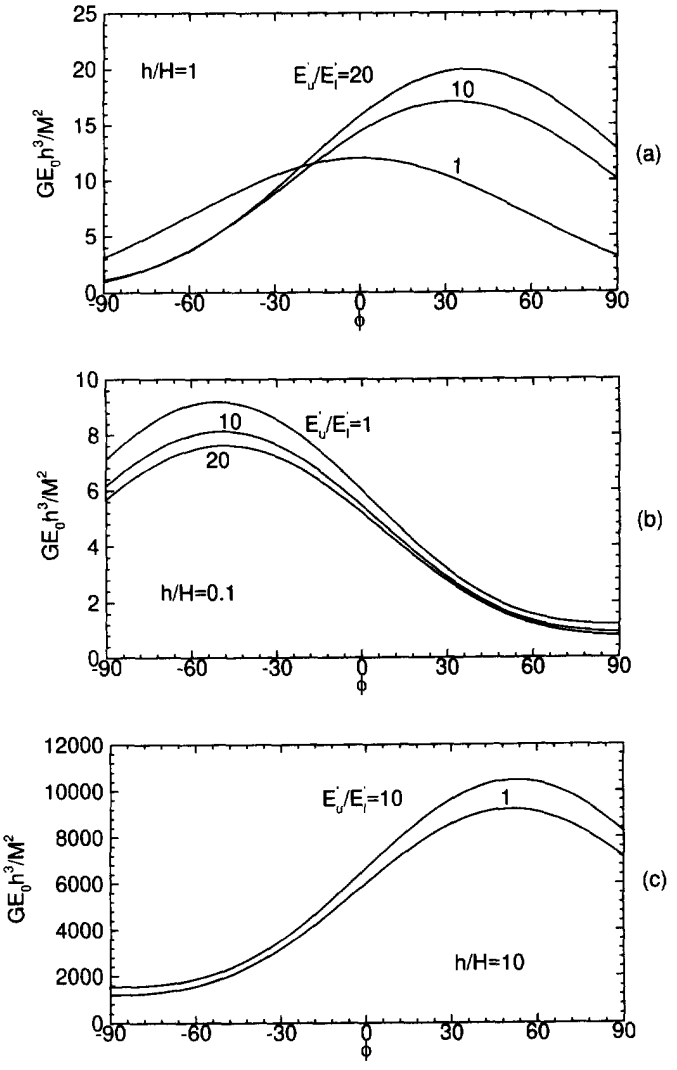


Fig. 5. The energy release rate for the double-cantilever beam for (a) $h/H = 1$, (b) $h/H = 0.1$ and (c) $h/H = 10$.

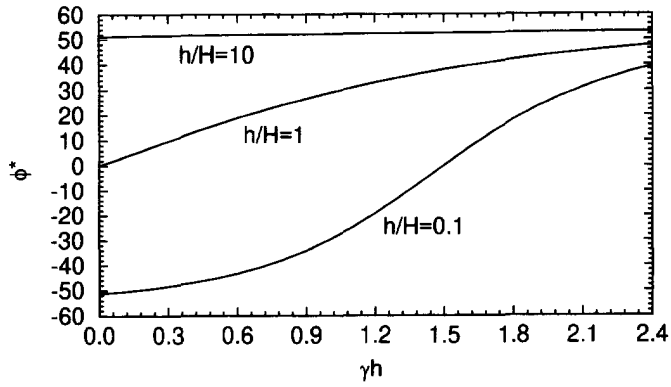


Fig. 6. Kink angle for the double-cantilever beam.

downwards (Fig. 2). When $h/H = 1$ (the crack is at the middle of the strip) and $h/H = 10$ (the crack is at the compliant side), the energy release rate is enhanced if $\phi > 0$; and it increases as the material gradient, measured by $E'_u/E'_l$, increases. When $h/H = 0.1$ (the crack is at the stiff side), the trend is different: the energy release rate is enhanced if $\phi < 0$; it decreases as the material gradient, $E'_u/E'_l$, increases. For some crack positions, the material gradient does have a strong effect on the energy release rate. For example, at $h/H = 1$, the maximum energy release rate for $E'_u/E'_l = 20$ is about 20, whereas it is 12 for the homogeneous case, $E'_u/E'_l = 1$. The implication of these qualitative behaviors is that when the crack is at the position where $h/H$ is sufficiently large, the crack is kinked to the more compliant side, or downwards; when the crack is at the position where $h/H$ is small, the crack is kinked to the stiffer side, or upwards. For the case of $h/H = 1$, the kink angle, the angle at which maximum energy release rate occurs, is $0^\circ$ for homogeneous materials. This is a well known result, and is due to the symmetric loading and symmetric material properties in this case. It is also seen that, for the cases of $h/H = 1$ and $h/H = 10$, the kink angle increases as the material gradient increases. Kink angles for the three crack positions are plotted in Fig. 6. It shows that for small $\gamma$, the kink angles for the three crack positions are quite different, but as $\gamma$ increases they become closer. When $h/H = 0.1$, the kink angle changes from negative sign to positive sign, i.e., upward kink becomes downward kink, at $\gamma h \approx 1.5$ as it increases. But at this crack position, it is seen from (20) that $E'_u/E'_l = 40$ for $\gamma h = 0.34$. This tells us that the portion of the curve where $\gamma h > 0.34$ is no practical use, since $E'_u/E'_l > 40$ in that portion and such large difference in elastic moduli may not appear in a FGM, at least, at the present time. It is noted that when the crack is at the middle position, the material gradient does have a strong effect on the kink angle, whereas it has little effect for the crack close to the upper and lower boundaries.

For the four-point bending specimen, it is assumed that the horizontal distance between the crack tip and the loading is large enough. As shown in Fig. 7, the maximum energy release rate is attained when $\phi$ is positive, and increases as the material gradient, $E'_u/E'_l$, increases for $h/H = 1$, 0.1 and 10. When $h/H = 0.1$ and 1, the increase of it is significant. For example, at $h/H = 0.1$, the energy release rate is 0.003 for the case of homogeneous materials, and 0.017 for $E'_u/E'_l = 20$; at $h/H = 1$, it is 8.41 and 20.02 for the two cases, respectively. Kink angles for the three crack positions are plotted vs the material gradient $\gamma h$ in Fig. 8. The figure shows, for the four-point bending specimen, $\gamma h$ does not have a strong effect on the kink angle. When the crack is at the middle of the beam, the difference of it between the case of a homogeneous material and that of $E'_u/E'_l = 20$ is less than $2^\circ$. When the crack is at $h/H = 0.1$ and 10 the difference is even less. In experiments, such small difference is difficult to be measured.

For the center cracked plate shown in Fig. 4(d), the energy release rate, besides $h/H$ and $\gamma h$, also varies with the crack length $a/h$. For the case of $a/h = 1$, kink angles are shown in Fig. 9. The trend of these curves is similar to that in Fig. 6 for the double-cantilever beam.

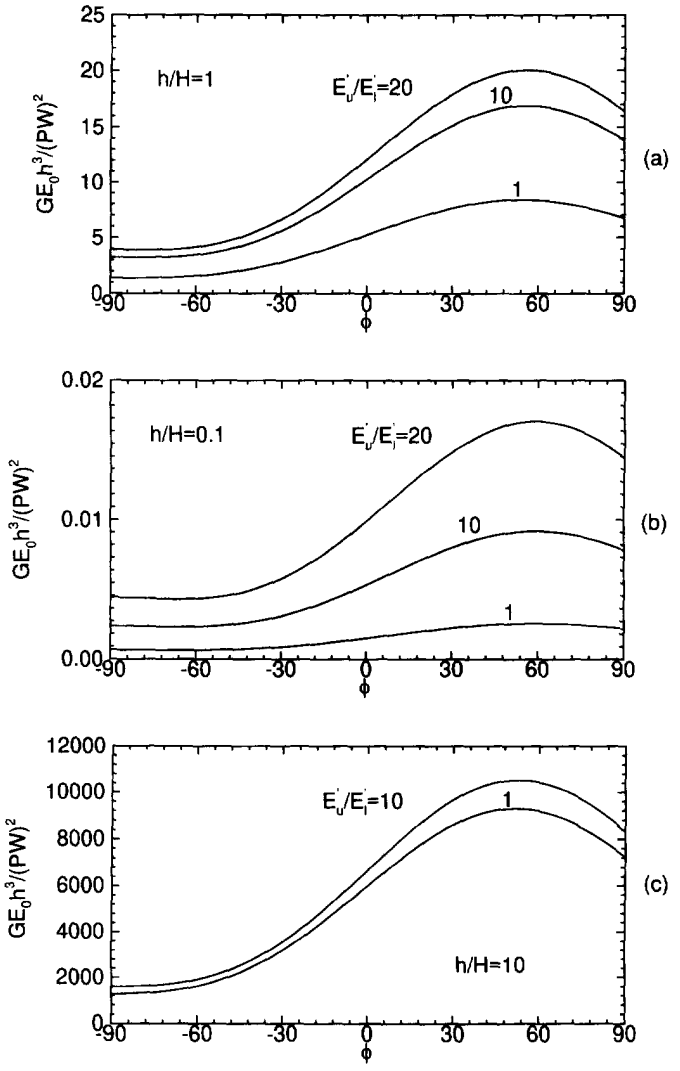


Fig. 7. The energy release rate for the four-point bending specimen for (a) $h/H = 1$, (b) $h/H = 0.1$ and (c) $h/H = 10$.

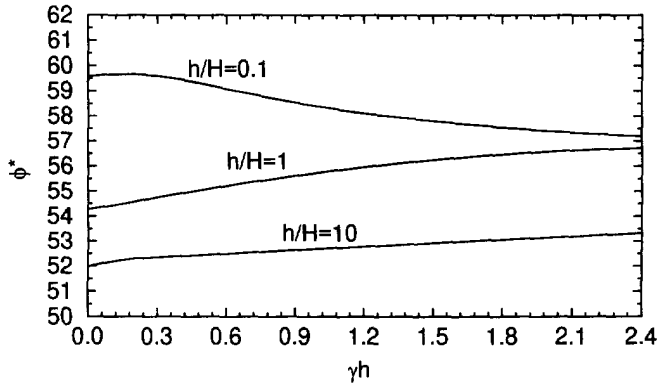


Fig. 8. Kink angle for the four-point bending specimen.

Two layers can be jointed by a compositionally graded material (FGM) sandwiched between them, as shown in Fig. 10. It reduces the mismatch of the bimaterial without the interlayer and gives better thermal-mechanical performance for the whole system (Giannakopoulos *et al.*, 1995). Also, for a bimaterial, the interface, the transition zone, is a FGM microscopically. For some bimaterials, the thickness of the zone is at the level that it may

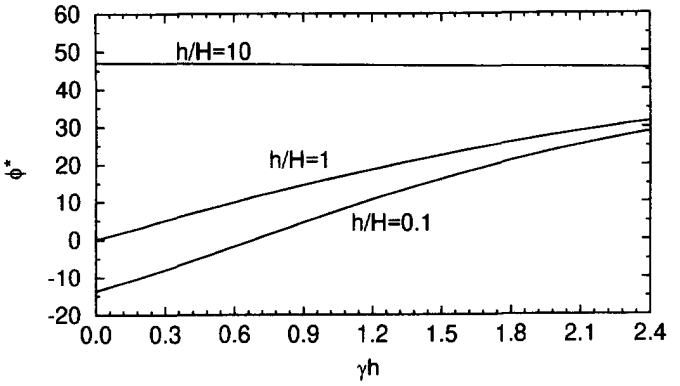


Fig. 9. Kink angle for the center cracked plate.

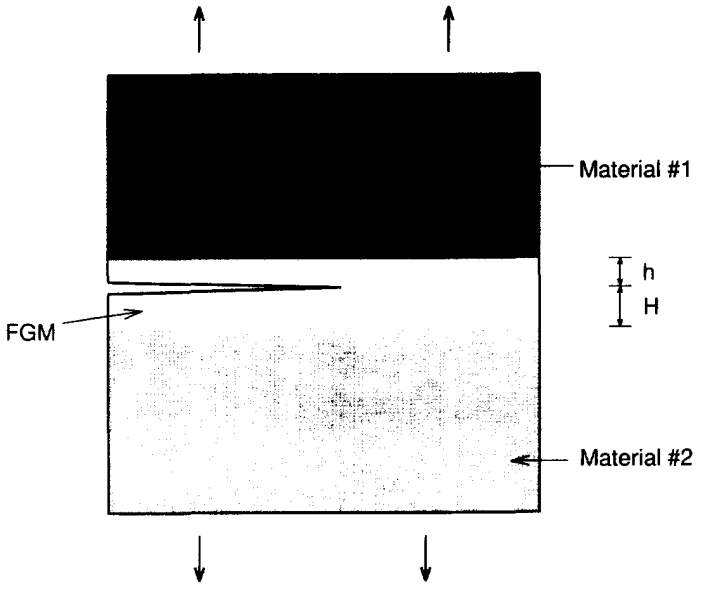


Fig. 10. A crack in a compositionally graded layer between two dissimilar materials.

not be neglected in analyzing the fracture of the interface. We use the above method to study the crack propagation inside the compositionally graded layer. The main crack shown in the above figure is parallel to the boundaries of the graded layer. The thicknesses of the two bulk materials are considered as much larger than the thickness of the interlayer. For a crack on a sharp interface, as discussed in Section 3.2, the energy release rate of the kinked crack is dependent on the extension length, and there is a contact zone in the region very close to the main crack tip due to its oscillatory singular field. The solution to the crack deflection problem in such case is not unique, except one of the two Dundurs' parameters, $\beta$, vanishes. It is seen that by introducing the transition zone to the interface the oscillatory singular field near the main crack tip, which is physically unacceptable, is removed, and therefore the problem of non-uniqueness for crack kinking does not exist.

The thickness of the graded layer and the position of the crack inside it are specified by $h$ and $H$ shown in Fig. 10. Here, since the thickness of the graded layer is considered much less than the length scale of the two bulk materials, the loading is represented by the complex stress intensity factor $K^{\infty}$ of the bimaterial problem without the graded layer. The complex stress intensity factor $K$ of the crack inside the graded layer is expressed as

$$K = q\, e^{i\omega} h^{i\varepsilon} K^{\infty}. \tag{21}$$

The equation is obtained by dimension analysis and linearity consideration. Both $q$ and $\omega$ in above expression are functions of Dundurs' parameters, $\alpha$ and $\beta$, the position of the

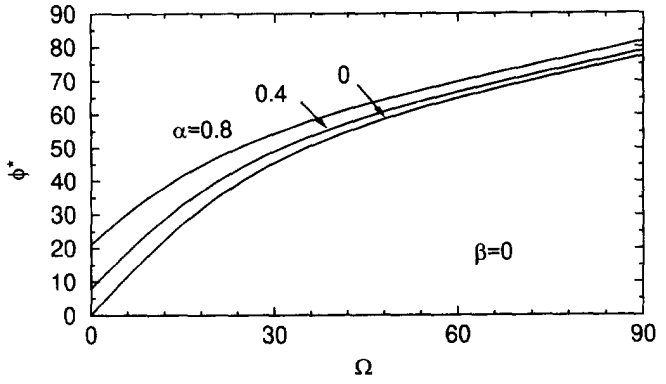


Fig. 11. The effect of $\alpha$ on kink angle for a crack inside the compositionally graded layer.

crack inside the graded layer, $h/H$, and the form of the material gradients. The former can be evaluated by using the $J$ integral. For the case that the elastic modulus follows the exponential form given in (18) and Poisson's ratio is a constant,

$$q = \frac{\sqrt{1-\beta^2}}{(1+\alpha)^{h/2(h+H)}(1-\alpha)^{H/2(h+H)}}. \tag{22}$$

For $h/H = 1$, Yang and Shih (1994) gave a general expression to estimate $\omega$ for any form of material property variation in terms of a known bimaterial solution. They compared the results obtained from the approximation with those from finite element analyses, and it was concluded that the approximation was quite satisfactory. We use their expression to examine crack deflection in the graded layer for the case where $h/H = 1$ and material properties follow the above mentioned form. In Fig. 11, we plot the kink angle for $\alpha = 0$, 0.4 and 0.8, where $\beta = 0$ and

$$\Omega = \arctan\frac{\mathrm{Im}(K^{\infty} h^{i\varepsilon})}{\mathrm{Re}(K^{\infty} h^{i\varepsilon})}. \tag{23}$$

The effect of $\alpha$ on the kink angle is stronger for small $\Omega$ than for large $\Omega$. In Fig. 12, we plot the kink angle for $\beta = 0$ and 0.2, where $\alpha = 0.4$. Since for many engineering materials $\beta$ is less than 0.2 (see Suga *et al.*, 1988), the two figures show that $\beta$ has a weaker effect on the kink angle than $\alpha$. The results which are obtained from the linear variation of the material properties also support the observation.

The current study provides a means to assess crack deflection in a special set of FGMs, simply nonhomogeneous materials. From the above solutions, it is seen that material gradients do have a strong effect on the kink direction when a crack is at the central part of the FGMs. The solutions may be used in either testing the fracture behavior or measuring

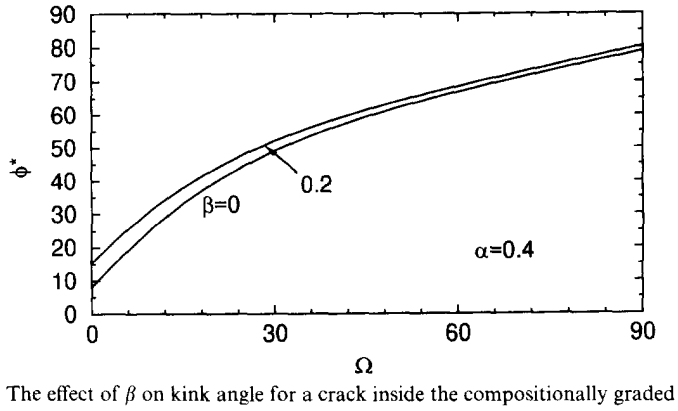


Fig. 12. The effect of $\beta$ on kink angle for a crack inside the compositionally graded layer.

the toughness of FGMs. On the other hand, this study can be viewed as an initial effort for crack deflection in real FGMs: the effect of microstructure, i.e., the effect of local inhomogeneities around the crack tip on both the energy release rate and the toughness, is up for further investigation.

*Acknowledgments*—This work was supported by the Office of Naval Research through Grant N00014-93-1-1164.

## REFERENCES

Barenblatt, G. I. (1962). The mathematical theory of equilibrium cracks in brittle fracture. *Advances in Applied Mechanics* **7**, 55–129.

Cotterell, B. (1965). On brittle fracture paths. *International Journal of Fracture* **1**, 96–103.

Cotterell, B. and Rice, J. R. (1980). Slightly curved or kinked cracks. *International Journal of Fracture* **16**, 155–169.

Dugdale, D. S. (1960). Yielding of steel sheets containing slits. *Journal of the Mechanics and Physics of Solids* **8**, 100–108.

Dundurs, J. (1969). Edge-bonded dissimilar orthogonal elastic wedges. *Journal of Applied Mechanics* **36**, 650–652.

Geubelle, P. H. and Knauss, W. G. (1994). Crack propagation at and near bimaterial interfaces: linear analysis. *Journal of Applied Mechanics* **61**, 560–566.

Giannakopoulos, A. E., Suresh, S., Finot, M. and Olsson, M. (1995). Elastoplastic analysis of thermal cycling: layered materials with compositional gradients. *Acta Metallurgica* **43**, 1335–1354.

Goldstein, R. V. and Salganik, R. L. (1974). Brittle fracture of solids with arbitrary cracks. *International Journal of Fracture* **10**, 507–523.

Gu, P. (1993). Multilayer material with an interface crack. *Journal of Applied Mechanics* **60**, 1052–1054.

Gu, P. and Asaro, R. J. (1997). Cracks in functionally graded materials. *International Journal of Solids and Structures* **34**, 1–17.

Gu, P. and Asaro, R. J. (1996). Plastic crack problems in functionally graded materials. Work in progress.

He, M.-Y. and Hutchinson, J. W. (1989). Kinking of a crack out of an interface. *Journal of Applied Mechanics* **56**, 270–278.

Holt, J. B., Koizumi, M., Hirai, T. and Munir, Z. A. (eds) (1993). *Ceramic Transactions* vol. 34, The American Ceramic Society, Westerville, Ohio.

Hutchinson, J. W. (1990). Mixed mode fracture mechanics of interfaces. In *Metal-Ceramic Interfaces, Acta-Scripta Metall. Proc.* Vol. 4, Pergamon, New York, pp. 295–306.

Lo, K. K. (1978). Analysis of branched cracks. *Journal of Applied Mechanics* **45**, 797–802.

Mukai, D. J., Ballarini, R. and Miller, G. R. (1990). Analysis of branched interface cracks. *Journal of Applied Mechanics* **57**, 887–893.

O'Dowd, N. P., Shih, C. F. and Stout, M. G. (1992). Test geometries for measuring interfacial fracture toughness. *International Journal of Solids and Structures* **29**, 571–589.

Palaniswamy, K. and Knauss, W. G. (1978). On the problem of crack extension in brittle solids under general loading. *Mechanics Today* Vol. 4, Pergamon, New York, pp. 87–148.

Rice, J. R. (1968). A path independent integral and approximate analysis of strain concentration by notches and cracks. *Journal of Applied Mechanics* **35**, 379–386.

Rice, J. R. (1988). Elastic fracture mechanics concepts for interfacial cracks. *Journal of Applied Mechanics* **55**, 98–103.

Shih, C. F. (1991). Cracks on bimaterial interfaces: elasticity and plasticity aspects. *Materials Science and Engineering* **A143**, 77–90.

Shih, C. F. and Asaro, R. J. (1988). Elastic-plastic analysis of cracks on bimaterial interfaces: part I—small scale yielding. *Journal of Applied Mechanics* **55**, 299–316.

Shih, C. F. and Asaro, R. J. (1989). Elastic-plastic analysis of cracks on bimaterial interfaces: part II—structure of small scale yielding fields. *Journal of Applied Mechanics* **56**, 763–779.

Suga, T., Elssner, E. and Schmander, S. (1988). Composite parameters and mechanical compatibility of material joints. *Journal of Computers and Materials* **22**, 917–934.

Symington, M. F. (1987). Eigenvalues for interface cracks in linear elasticity. *Journal of Applied Mechanics* **54**, 973–974.

Yamanouchi, M., Koizumi, M., Hirai, T. and Shiota, I. (eds) (1990). *Proceedings of the First International Symposium on Functionally Gradient Materials*, Sendai, Japan.

Yang, W. and Shih, C. F. (1994). Fracture along an interlayer. *International Journal of Solids and Structures* **31**, 985–1002.